J Physiol 596.6 (2018) pp 1019–1033

The Journal of Physiology

The large-conductance voltage- and Ca^{2+}-activated K^+ channel and its γ1-subunit modulate mouse uterine artery function during pregnancy

Ramón A. Lorca, Monali Wakle-Prabagaran, William E. Freeman, Meghan K. Pillai and Sarah K. England

Center for Reproductive Health Sciences, Department of Obstetrics and Gynecology, Washington University in St Louis School of Medicine, St Louis, MO 63110, USA

Edited by: Laura Bennet & Kim Dora

Key points

- The uterine artery (UA) markedly vasodilates during pregnancy to direct blood flow to the developing fetus. Inadequate UA vasodilatation leads to intrauterine growth restriction and fetal death.
- The large-conductance voltage- and Ca^{2+}-activated K^+ (BK_{Ca}) channel promotes UA vasodilatation during pregnancy.
- We report that BK_{Ca} channel activation increases the UA diameter at late pregnancy stages in mice.
- Additionally, a BK_{Ca} channel auxiliary subunit, γ1, participates in this process by increasing channel activation and inducing UA vasodilatation at late pregnancy stages.
- Our results highlight the importance of the BK_{Ca} channel and its γ1-subunit for UA functional changes during pregnancy.

Abstract Insufficient vasodilatation of the uterine artery (UA) during pregnancy leads to poor utero-placental perfusion, contributing to intrauterine growth restriction and fetal loss. Activity of the large-conductance Ca^{2+}-activated K^+ (BK_{Ca}) channel increases in the UA during pregnancy, and its inhibition reduces uterine blood flow, highlighting a role of this channel in UA adaptation to pregnancy. The auxiliary γ1-subunit increases BK_{Ca} activation in vascular smooth muscle, but its role in pregnancy-associated UA remodelling is unknown. We explored whether the BK_{Ca} and its γ1-subunit contribute to UA remodelling during pregnancy. Doppler imaging revealed that, compared to UAs from wild-type (WT) mice, UAs from BK_{Ca} knockout ($BK_{Ca}^{-/-}$) mice had lower resistance at pregnancy day 14 (P14) but not at P18. Lumen diameters were twofold larger in pressurized UAs from P18 WT mice than in those from non-pregnant mice, but this difference was not

Ramón A. Lorca received his PhD in Physiology from the P. Catholic University of Chile in 2008. He did postdoctoral training at the University of Iowa and Washington University in St Louis. He is currently an instructor in the Department of Obstetrics and Gynecology at the University of Colorado Denver. His research interests focus on the regulation of vascular and uterine smooth muscle cell excitability during pregnancy.

DOI: 10.1113/JP274524

seen in UAs from $BK_{Ca}^{-/-}$ mice. UAs from pregnant WT mice constricted 20–50% in response to the BK_{Ca} blocker iberiotoxin (IbTX), whereas UAs from non-pregnant WT mice only constricted 15%. Patch-clamp analysis of WT UA smooth muscle cells confirmed that BK_{Ca} activity increased over pregnancy, showing three distinct voltage sensitivities. The γ1-subunit transcript increased 7- to 10-fold during pregnancy. Furthermore, γ1-subunit knockdown reduced IbTX sensitivity in UAs from pregnant mice, whereas γ1-subunit overexpression increased IbTX sensitivity in UAs from non-pregnant mice. Finally, at P18, γ1-knockout ($\gamma1^{-/-}$) mice had smaller UA diameters than WT mice, and IbTX-mediated vasoconstriction was prevented in UAs from $\gamma1^{-/-}$ mice. Our results suggest that the γ1-subunit increases BK_{Ca} activation in UAs during pregnancy.

(Received 18 April 2017; accepted after revision 5 January 2018; first published online 10 January 2018)
Corresponding author R. A. Lorca: Division of Reproductive Sciences, Department of Obstetrics and Gynecology, University of Colorado Denver, 12700 E. 19th Avenue, Mail Stop 8613, Research Complex II, Room 3101, Aurora, CO 80045, USA. Email: ramon.lorca@ucdenver.edu

Introduction

Fetal growth and development require a progressive increase in maternal utero-placental circulation. Insufficient utero-placental perfusion contributes to adverse pregnancy outcomes such as intrauterine growth restriction (IUGR), pre-eclampsia and fetal loss (Chiswick, 1985; Konje *et al.* 2003; Browne *et al.* 2011; Rada *et al.* 2012; Cotechini *et al.* 2014; Janot *et al.* 2014). A major mechanism for increasing blood flow to the placenta is vasodilatation and remodelling of the uterine artery (UA) (Ford, 1982; Palmer *et al.* 1992; Osol & Cipolla, 1993; Hilgers *et al.* 2003; Mu & Adamson, 2006). Thus, during pregnancy, the UA diameter significantly increases (Osol & Cipolla, 1993; Cipolla & Osol, 1994) and UA resistance decreases (Ford, 1982; Palmer *et al.* 1992; Mu & Adamson, 2006).

One key player in pregnancy-dependent increases in uterine blood flow is the large-conductance voltage- and Ca^{2+}-activated K^+ (BK_{Ca}) channel. Blocking BK_{Ca} channels reduces blood flow in UAs from pregnant sheep (Rosenfeld *et al.* 2001), and BK_{Ca} channel currents increase in sheep UA smooth muscle cells (SMCs) during pregnancy, although the BK_{Ca} protein expression level remains constant over pregnancy (Rosenfeld *et al.* 2009; Hu *et al.* 2011). In addition, BK_{Ca} channels regulate vascular function in UAs from non-pregnant women (Rosenfeld *et al.* 2008), suggesting an evolutionarily conserved role in regulating UA function.

BK_{Ca} channel activation can be regulated by numerous mechanisms, such as membrane microdomain localization (Brainard *et al.* 2005; Alioua *et al.* 2008; Lu *et al.* 2010), alternative splicing (Korovkina *et al.* 2001; Curley *et al.* 2004; Zhu *et al.* 2005), and association with modulatory subunits (Knaus *et al.* 1994; Tanaka *et al.* 1997; Brenner *et al.* 2000; Yan & Aldrich, 2012; Evanson *et al.* 2014). Auxiliary subunits are proposed to confer cell- or tissue-specific functional diversity. In vascular SMCs, the β1-subunit enhances voltage activation and apparent Ca^{2+} sensitivity of the BK_{Ca} channel (McManus *et al.* 1995; Tanaka *et al.* 1997; Brenner *et al.* 2000). Moreover, expression of the BK_{Ca} channel β1-subunit is higher in UAs from pregnant sheep than in those from non-pregnant animals (Rosenfeld *et al.* 2009; Hu *et al.* 2011). This finding suggests that the β1-subunit participates in the increased activity of BK_{Ca} channels in UA SMCs during pregnancy and may explain why BK_{Ca} activity increases even though expression level does not change (Rosenfeld *et al.* 2009; Hu *et al.* 2011).

Recent studies have revealed that, in addition to β-subunits, BK_{Ca} channels associate with γ-subunits (Yan & Aldrich, 2010, 2012). The first described member of this family, the γ1-subunit (also referred to as the leucine-rich repeat-containing protein 26), markedly increases the voltage sensitivity of the BK_{Ca} channel, activating it at resting membrane potentials, without a rise in intracellular Ca^{2+} (Yan & Aldrich, 2010). The γ1-subunit is expressed in cerebral artery SMCs, where it modulates BK_{Ca} channel activity and reduces myogenic tone (Evanson *et al.* 2014). However, whether the γ1-subunit regulates BK_{Ca} channel activity in other vascular beds has not been explored.

Here, we tested the hypothesis that the γ1-subunit increases BK_{Ca} channel activity in UA SMCs during pregnancy. We observed that UAs from BK_{Ca} channel knockout ($BK_{Ca}^{-/-}$) mice had lower *in vivo* resistance and smaller *in vitro* diameter during pregnancy than those from wild-type (WT) mice. Pharmacological blockade and single-channel analysis of BK_{Ca} currents in UA SMCs indicated that BK_{Ca} activity and voltage sensitivity increased over the course of mouse pregnancy. Moreover, the increased BK_{Ca} channel activity in UAs from pregnant mice was reduced by knockdown of the γ1-subunit. Finally, γ1-subunit knockout mice exhibited reduced UA diameter and BK_{Ca} channel activity during pregnancy. Our findings suggest that the γ1-subunit contributes to the pregnancy-dependent increase in BK_{Ca} channel activity in the UA.

Methods

Mice

All animal work complied with the *Guidelines for the Care and Use of Laboratory Animals* set forth by the NIH and protocols approved by the Animal Care and Use Committee at Washington University in St Louis School of Medicine. $BK_{Ca}^{-/-}$ mice (a gift from Dr Andrea L. Meredith at University of Maryland) have stable, germ line-transmissible deletion of exon 1 of the *mSlo1* gene (Meredith *et al.* 2004). Because $BK_{Ca}^{-/-}$ males exhibit a significantly lower mating efficiency than WT mice, the mouse colony was maintained by breeding heterozygous mice. Genotyping was performed by PCR of tail DNA with the following primers: 5′-TTCATCATCTTGCTCTGGCGGACG-3′, 5′-CCATAG TCACCAATAGCCC-3′, 5′-ATAGCCTGAAGAACGAGAT CAGC-3′ and 5′-CCTCAAGAAGGGGACTCTAAAC-3′, and confirmed by Transnetyx, Inc. (Cordova, TN, USA). Eight- to-twelve-week-old homozygous $BK_{Ca}^{-/-}$ females and their WT littermates were mated to WT males, resulting in $BK_{Ca}^{+/-}$ and WT offspring, respectively. Mice lacking the *lrrc26* gene ($\gamma1^{-/-}$) were kindly provided by Dr Christopher Lingle (Washington University in St Louis) (Yang *et al.* 2017), and the colony was maintained as homozygous mutants. Day 0 of pregnancy was determined by the presence of a copulatory plug after mating for 2–3 h. Mice were killed by gradually increasing the CO_2 flow rate into the chamber and then performing cervical dislocation. Primary UAs from both uterine arcades were dissected from non-pregnant (NP) mice and from pregnant mice on days 14 (P14, after placentation) and 18 (P18, before labour initiation). After the dams were killed, the numbers of live pups were recorded, and pups were killed by decapitation.

Blood flow and embryonic measurements

P14 and P18 $BK_{Ca}^{-/-}$ and WT mice were sedated by subcutaneous administration of 1.2–5 mg midazolam. Mice remained awake but docile. *In vivo* analysis of blood flow was conducted with an Acuson Sequoia c256 echocardiographic system (Acuson Corp., Mountain View, CA, USA) fitted with a 15 MHz linear array oscillator/receiver. A 40 MHz linear array probe was applied to the chest to measure maternal heart rate and other cardiac parameters. The imaging probe was coupled to a Vevo 2100 imaging system (VisualSonics, Toronto, ON, Canada), generating ∼180–200 two-dimensional frames per second. Uterine and fetal sonography was performed by applying the probe to the lower abdomen. Two-dimensional sonographic images were used to measure crown–rump length (fetal size), placental thickness at the point of umbilical cord insertion, and fetal heart rate. All values were averaged from three pups per dam. Pulse-wave Doppler evaluation was used to measure flow velocity in UAs adjacent to the gestational sacs and umbilical arteries. UA resistance index ((PSV − EDV)/PSV, where PSV is peak systolic velocity and EDV is end-diastolic velocity) and UA pulsatility index ((PSV − EDV)/time-averaged maximum velocity) were calculated as indicators of vascular resistance downstream of the UA. All sonographic images were analysed by an investigator blinded to the mouse genotype. After at least 1 h of recovery from sedation, P14 mice were housed until P18, when another ultrasound was performed. After at least 1 h of recovery from sedation after P18 ultrasound, vascular function was assessed in some of the mice.

Immunohistochemistry

P18 UAs were dissected in ice-cold Dulbecco's phosphate buffered saline (Gibco, Carlsbad, CA, USA) and immediately fixed in 4% paraformaldehyde (Affymetrix, Cleveland, OH, USA) for 24 h at 4°C, embedded in 2% agar (Sigma-Aldrich, St Louis, MO, USA), and then embedded in paraffin. Sections (5 μm) were adhered to slides, deparaffinized with xylenes (Sigma-Aldrich), and rehydrated. Slides were treated with a citrate-based solution (Vector Laboratories, Burlingame, CA, USA) for antigen retrieval and then stained with rabbit anti-BK_{Ca} α (Abcam, Eugene, OR, USA, 1:100) or rabbit anti-CD31 (Cell Signaling Technology, Danvers, MA, USA, 1:50) and wheat germ agglutinin (Alexa 555 conjugate, Invitrogen, Grand Island, NY, USA), mounted, and then imaged with a Nikon Diaphot fluorescence microscope.

Vascular function

UAs were dissected as described above, cannulated onto glass cannulas filled with Krebs solution (118 mM NaCl, 4.7 mM KCl, 2.5 mM $CaCl_2$, 1.2 mM $MgSO_4$, 1.2 mM KH_2PO_4, 25 mM $NaHCO_3$, and 11 mM glucose), a common buffer used in physiological studies (Gutkowska *et al.* 1997; Knot & Nelson, 1998; Cheranov & Jaggar, 2004; Ketsawatsomkron *et al.* 2012), and secured with sutures in a Pressure Myograph System 110P (DMT-USA, Ann Arbor, MI, USA). Oxygenated (95% O_2 and 5% CO_2) and warmed (37°C) Krebs buffer was continuously circulated through the chamber. Using a split-screen microscope connected to a video camera, lumen and outer vascular diameters were continuously recorded with MyoVIEW software (DMT-USA). Main UAs were pressurized to 60 mmHg (Hilgers *et al.* 2003) and allowed to equilibrate for a minimum of 45 min before study. To ensure viability, 50 mM KCl was added from a 2 M stock solution at the beginning and end of each experiment, and data were discarded if UAs showed <40% reduction of basal diameter in the presence of 50 mM KCl. Similar contractile responses were seen when Krebs was instead

substituted with a high-K^+/low-Na^+ Krebs solution (R. A. Lorca, unpublished observations). Iberiotoxin (IbTX, Tocris, Bristol, UK) was sequentially applied at 1–100 nM in the presence of a low KCl concentration (15 mM), which slightly depolarizes SMCs, inducing an increase of intracellular Ca^{2+} and activating BK_{Ca} channels. The endothelium was removed before each experiment by passing air bubbles through the lumen and then flushing with Krebs buffer. As previously described (Ketsawatsomkron *et al.* 2012), endothelial removal was confirmed by detecting <30% vasorelaxation in the presence of 10 μM acetylcholine (Sigma-Aldrich) in vessels pre-constricted with 15 mM KCl. Lumen and external diameters of UAs pressurized at 60 mmHg in regular Krebs buffer but with no other stimulation were used to calculate wall thickness, cross-sectional area and wall:lumen ratio.

Vascular SMC isolation

Single SMCs were enzymatically dissociated from UAs as described previously (Jackson *et al.* 1997). Briefly, isolated UAs were placed in ice-cold Dulbecco's phosphate buffered saline, then cut into ≤2 mm-long segments and incubated for 10 min at room temperature in dissociation solution (DS) containing (in mM): 145 NaCl, 4 KCl, 0.05 $CaCl_2$, 1 $MgCl_2$, 10 HEPES, 10 glucose (pH 7.4 with NaOH), and 0.1% bovine serum albumin (RPI, Mount Prospect, IL, USA). Then, the pieces were placed in DS containing (in mg ml^{-1}): 1.5 papain (Worthington Biochemical, Lakewood, NJ, USA) and 1 dithiothreitol (Sigma-Aldrich), and incubated at 37°C for 25 min. Next, the solution was replaced with DS containing (in mg ml^{-1}): 1.5 collagenase type H (Sigma-Aldrich), 1 trypsin inhibitor, and 0.5 elastase (both from Worthington Biochemical) and incubated at 37°C for 5 min. Pieces were incubated for 3 min at room temperature and then placed on ice for 5 min. After digestion, the pieces were gently triturated in ice-cold DS until elongated vascular SMCs were observed. SMCs were placed on glass coverslips and allowed to attach for at least 40 min at 4°C before electrophysiological experiments were performed.

Electrophysiology

Excised-patch recordings in the inside-out configuration were performed on isolated SMCs at room temperature in a bath solution containing (in mM): 140 KCl, 20 KOH, 10 HEPES, 5 (H)EDTA, and 10 μM free-Ca^{2+} (pH 7.2 with HCl). Free-Ca^{2+} concentration was measured with a Ca^{2+}-sensitive electrode (Thermo Fisher Scientific, Rockford, IL, USA). The pipette solution contained (in mM): 140 KCl, 20 KOH, 2 $MgCl_2$, and 10 HEPES (pH 7.4 with HCl). Single-channel currents were recorded at a sampling rate of 100 kHz and filtered at 5 kHz by using an Axopatch 200B amplifier (Molecular Devices, Sunnyvale, CA, USA). pCLAMP 10 software (Molecular Devices) was used to evoke currents with 10 mV voltage steps (1000 ms duration) from −120 to +100 mV, from a holding potential of 0 mV. Mean open probability (P_o) values were calculated with pCLAMP 10 software. Half-maximal activation voltage ($V_{0.5}$) values were determined for each experiment by using GraphPad 6 software (San Diego, CA, USA) to fit membrane potential (V) to a Boltzmann function, $P_o = P_{o(max)}/(1 + e^{-zF(V - V_{0.5})/RT})$, where z is the effective charge, F is the Faraday constant, R is the ideal gas constant, and T is temperature.

RNA isolation and quantitative PCR

Total RNA from isolated UAs was extracted by using an Arcturus PicoPure RNA isolation kit (Thermo Fisher Scientific) and reverse transcribed with iScript reverse transcription supermix (Bio-Rad, Hercules, CA, USA) according to the manufacturers' instructions. The CFX96 Real-time System with IQ-SYBR Green Supermix (Bio-Rad) was used for real-time PCR. The primer sequences (Integrated DNA Technologies, Coralville, IA, USA) were: mouse BK_{Ca} α-subunit (GenBank accession no: NM_010610.2), 5′-AGATCGACATGGCTTTCAA-3′ and 5′-CAGGAGGGACTGTGAAGA-3′; mouse BK_{Ca} β1-subunit (NM_031169.4), 5′-CTGGGAGTGGCAATGGT AGT-3′ and 5′-GCCCACAGCTGATACATTGA-3′; mouse BK_{Ca} γ1-subunit (NM_146117.2), 5′-AAACTGAGACCC TGCTCTGC-3′ and 5′-GATGGCCAAACTAGCAAGGA-3′; mouse succinate dehydrogenase complex flavoprotein subunit A (SDHA, NM_023281), 5′-GGAACACTCCAA AAACAGACCT-3′ and 5′-CCACCACTGGGTATTGAG TAGAA-3′. Thermal cycling conditions were as follows: 95°C for 3 min, followed by 40 cycles of amplification at 95°C for 10 s and 57°C for 30 s. All samples were analysed in triplicate; mRNA data are reported relative to SDHA.

Transfection of intact UAs

Isolated UAs were placed in ice-cold Krebs buffer and reversibly permeabilized as described previously (Lesh *et al.* 1995). Briefly, UAs were placed for 20 min at 4°C in a solution containing (in mM): 120 KCl, 2 $MgCl_2$, 10 EGTA, 5 Na_2ATP, and 20 TES (pH 6.8 with KOH). After permeabilization, UAs were incubated for 90 min at 4°C in a similar buffer devoid of EGTA and containing 5 μg of non-targeting (scrambled, Scr) control short hairpin RNA (shRNA) or γ1-targeted shRNA in the pLKO vector (The Genome Institute, Washington University in St Louis, St Louis, MO, USA) for knockdown experiments. For overexpression experiments, UAs were incubated with 5 μg of either a pBudCE4.1 vector (Invitrogen) expressing the BK_{Ca} γ1-subunit (GenBank accession number: NM_146117.2) or an empty pBudCE4.1 vector. In both cases, the $MgCl_2$ concentration was then raised

Table 1. Maternal and fetal characteristics at P14 and P18

	WT dams			$BK_{Ca}^{-/-}$ dams			
	P14 (10)	P18 (11)	*P* P14 *vs.* P18	P14 (5)	P18 (6)	*P* P14 *vs.* P18	*P* WT *vs.* $BK_{Ca}^{-/-}$
Maternal heart rate (beats min^{-1})	555 ± 8	564 ± 6	NS	555 ± 15	575 ± 10	NS	NS
Relative wall thickness	0.5 ± 0.02	0.49 ± 0.02	NS	0.53 ± 0.02	0.51 ± 0.03	NS	NS
Fractional shortening (%)	46 ± 1	45 ± 2	NS	50 ± 1	44 ± 2	NS	NS
Ejection time (ms)	43.4 ± 0.6	42.7 ± 1.2	NS	41.9 ± 1.7	43.3 ± 2.3	NS	NS
UA PSV (mm s^{-1})	413 ± 50	447 ± 43	NS	420 ± 39	516 ± 51	NS	NS
UA EDV (mm s^{-1})	151 ± 17	237 ± 22	<0.05	237 ± 24	270 ± 27	NS	<0.05 at P14
UA TAmax velocity (mm s^{-1})	238 ± 27	296 ± 28	NS	272 ± 23	336 ± 33	NS	NS
	WT pups			$BK_{Ca}^{+/-}$ pups			
Number of pups per litter	8.6 + 0.2 [5]	8.6 + 0.3 [18]	NS	5.3 + 1 [6]	7 + 0.4 [7]	NS	<0.05 at P14 and P18
Crown–rump length (mm)	10.7 ± 0.3	16.8 ± 0.5	<0.05	10.3 ± 0.4	16.2 ± 0.6	<0.05	NS
Placental thickness (mm)	2.6 ± 0.2	2.8 ± 0.2	NS	2.4 ± 0.2	3.3 ± 0.1	<0.05	NS
Fetal heart rate (beats min^{-1})	186.8 ± 5.7	243.3 ± 7.1	<0.05	207.6 ± 12.0	230.3 ± 6.5	NS	NS
UmbA TAmax velocity (mm s^{-1})	126 ± 7	166 ± 10	<0.05	124 ± 7	167 ± 6	<0.05	NS

Data are means ± SEM. Number of dams are in parentheses, and in brackets where values were different. EDV, end-diastolic velocity; PSV, peak systolic velocity; TAmax, time-averaged maximum velocity; UmbA, umbilical artery. Significance columns (*P*) indicate differences between pregnancy stages or genotypes. NS, not significant. Two-way ANOVA, Sidak.

to 10 mM for 30 min, permeabilization was reversed by placing the UAs in a MOPS-buffered solution containing (in mM): 140 NaCl, 5 KCl, 10 $MgCl_2$, 5 glucose, and 2 MOPS (pH 7.1 with NaOH) at room temperature for 30 min, $[Ca^{2+}]$ was gradually increased from nominally Ca^{2+}-free to 0.01, 0.1 and 1.8 mM over a 45 min period, and then the UAs were incubated at 37°C in serum- and HEPES-free Dulbecco's modified Eagle medium (DMEM; Invitrogen) for 48–60 h.

Statistical analyses

The numbers of pups per litter and data obtained from Doppler ultrasound and vascular reactivity experiments were subjected to two-way ANOVA followed by Sidak's multiple comparison test (GraphPad 6 software). Patch-clamp and quantitative PCR (qPCR) experiments were analysed by non-parametric Kruskal–Wallis one-way ANOVA (GraphPad 6 software). A P value < 0.05 was considered significant.

Results

Maternal and fetal characteristics

$BK_{Ca}^{-/-}$ dams had significantly fewer pups per litter than WT dams (Table 1). There were no differences between genotypes in pup size measured as crown–rump length by ultrasound (Table 1). However, placental thickness increased from P14 to P18 in $BK_{Ca}^{-/-}$ dams but not in WT dams (Table 1). WT dams showed significant decreases in UA resistance index (RI) from P14 to P18 (0.62 ± 0.03 *vs.* 0.47 ± 0.02, $P < 0.01$, Fig. 1*A* and *B*), and in pulsatility index (PI) from P14 to P18 (1.09 ± 0.08 *vs.* 0.73 ± 0.04, $P < 0.01$, Fig. 1*A* and *C*), suggesting greater downstream dilatation and utero-placental blood flow. The decreases in UA RI and PI from P14 to P18 did not occur in the $BK_{Ca}^{-/-}$ dams (RI, 0.43 ± 0.03 in P14 and 0.48 ± 0.02 in P18; and PI, 0.67 ± 0.06 in P14 and 0.74 ± 0.04 in P18, Fig. 1*A*–*C*). Both RI and PI were lower at P14 in $BK_{Ca}^{-/-}$ dams than in WT dams ($P < 0.01$, Fig. 1*A*–*C*). The lower RI and PI in P14 $BK_{Ca}^{-/-}$ mice were associated with higher end-diastolic velocities rather than lower peak systolic velocities (Fig. 1*D* and *E*). Other maternal (WT *vs.* $BK_{Ca}^{-/-}$) or fetal (WT *vs.* $BK_{Ca}^{+/-}$) haemodynamic indices did not differ between genotypes (Table 1).

UA diameter and BK_{Ca} channel activity during pregnancy

To better understand how the BK_{Ca} channel alters the vascular parameters observed in Fig. 1, we isolated UAs from WT and $BK_{Ca}^{-/-}$ dams and performed immunofluorescence to determine where BK_{Ca} was expressed. We observed BK_{Ca} protein in the SMC layer (Fig. 2*A*) but not in the endothelial layer, which expressed the endothelial cell adhesion marker CD31 (Fig. 2*B*). As expected, BK_{Ca} staining intensity was decreased in UAs from $BK_{Ca}^{-/-}$ mice (Fig. 2*C*).

To examine the role of SMC BK_{Ca} in control of UA diameter, we isolated UAs and removed the endothelium, which has a role in UA adaptation during pregnancy (Bird *et al.* 2000). In UAs from WT mice, diameter increased progressively between NP, P14 and P18 (281 ± 19.2 μm, 448.3 ± 24.8 μm and 584.1 ± 18.1 μm, $P < 0.05$, Fig. 3*A*). In UAs from $BK_{Ca}^{-/-}$ mice, diameter increased between NP and P14 (266.5 ± 13.9 μm and 447.1 ± 6.9 μm, respectively, $P < 0.05$), but was not larger at P18 (433.2 ± 17.9 μm, Fig. 3*A*). Moreover, mean diameter was significantly smaller in UAs from $BK_{Ca}^{-/-}$ mice than in those from WT mice at P18 (433.2 ± 17.9 μm *vs.* 584.1 ± 18.1 μm, $P < 0.05$, Fig. 3*A*), indicating a role for BK_{Ca} channels in regulating UA smooth muscle basal tone during late pregnancy stages.

To determine whether BK_{Ca} contributed to UA architecture, we assessed wall thickness, cross-sectional area and wall:lumen ratio. Consistent with previous findings (van der Heijden *et al.* 2005), UAs from P14 and P18 mice had thicker walls than those from NP mice (Table 2). However, we did not see this increase in wall thickness between NP and P14 or P18 in UAs from $BK_{Ca}^{-/-}$ mice (Table 3). In WT mice, the wall:lumen ratio was lower in UAs from P18 than in those from P14 or NP (Table 2), but this difference was not observed in UAs from $BK_{Ca}^{-/-}$ mice (Table 3). Despite these differences, wall:lumen ratio, cross-sectional area and wall thickness did not differ significantly between UAs from WT and $BK_{Ca}^{-/-}$ mice at any stage (Tables 2 and 3).

Because loss of BK_{Ca} affected UA diameter but had no effect on any structural measures, we wondered whether BK_{Ca} contributed to UA contraction in response to KCl-mediated depolarization. We found that 15 mM KCl induced similar levels of constriction in UAs from NP, P14 and P18 WT mice (19.8 ± 3.8%, 17 + 3.9% and 32.2 ± 8.1% constriction, Fig. 3*B*). In contrast, 15 mM KCl induced a larger constriction in UAs from P14 and P18 $BK_{Ca}^{-/-}$ mice than in those from NP $BK_{Ca}^{-/-}$ mice (37.2 ± 8.5% and 38.4 ± 4.9% *vs.* 12.4 ± 5.1% constriction, $P < 0.05$, Fig. 3*B*), suggesting that BK_{Ca}

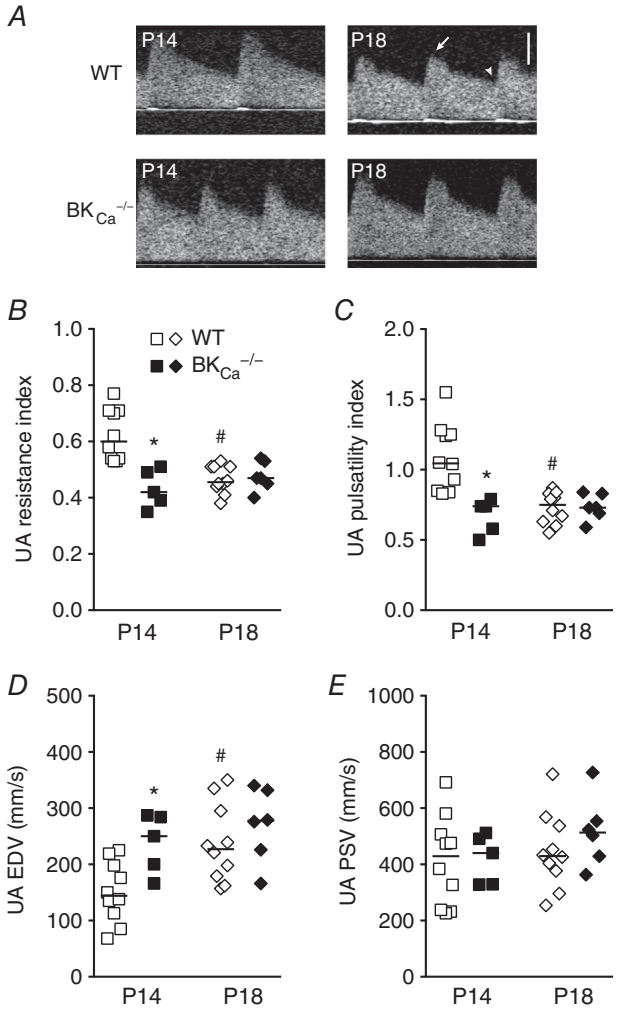

Figure 1. Doppler measurements in UAs from pregnant WT and $BK_{Ca}^{-/-}$ mice
A, Doppler flow velocity waveforms obtained in UAs from WT and $BK_{Ca}^{-/-}$ mice at P14 and P18. Arrow and arrowhead indicate peak systolic velocity (PSV) and end-diastolic velocity (EDV), respectively. Bar = 200 mm s^{-1}. *B–E*, Doppler imaging measurements of resistance index (*B*), pulsatility index (*C*), EDV (*D*) and PSV (*E*) in UAs from WT (open symbols, $n = 10$–11) and $BK_{Ca}^{-/-}$ mice (filled symbols, $n = 5$–6) at P14 and P18. Symbols represent individual values; bars represent median values. $^{*}P < 0.05$ compared to WT at same stage, $^{\#}P < 0.05$ compared to same genotype at P14.

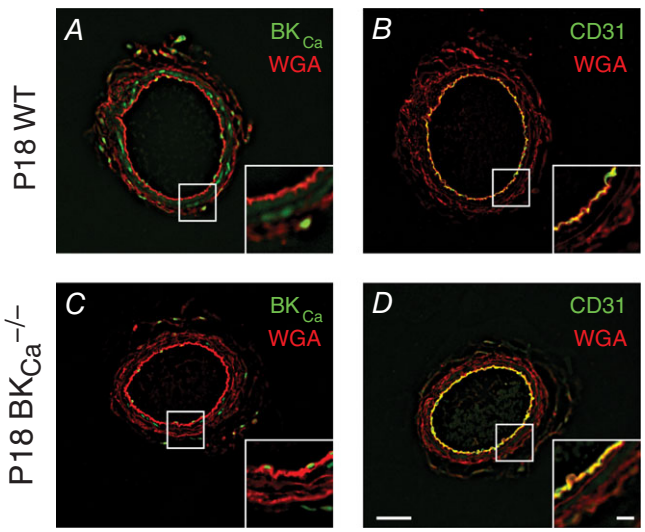

Figure 2. BK_{Ca} channel expression in UAs
Immunohistochemistry showing expression of BK_{Ca} channel (green) in non-pressurized P18 UAs from WT (*A*) and $BK_{Ca}^{-/-}$ (*C*) mice. CD31 (green) was used as an endothelial layer marker (*B* and *D*). Wheat germ agglutinin (WGA, red) was used to highlight vessel structure in all panels. Insets show high-magnification views of boxed areas. Bars = 50 μm and 10 μm (insets).

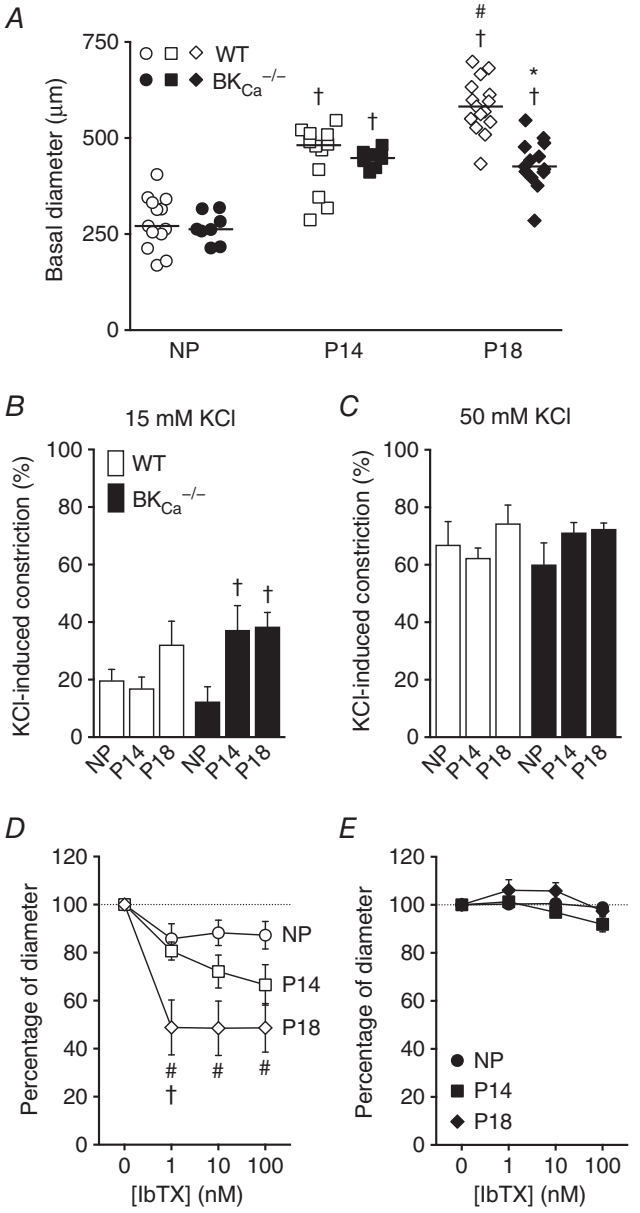

Figure 3. UA lumen diameter and BK$_{Ca}$ activity in UAs from WT and BK$_{Ca}^{-/-}$ mice
A, basal lumen diameter of pressurized UAs (60 mmHg) from NP, P14 and P18 WT (open symbols) and BK$_{Ca}^{-/-}$ (filled symbols) mice. Symbols are individual values; bars are median values. $^{\dagger}P < 0.05$ compared to NP of same genotype, $^{\#}P < 0.05$ compared to P14 of same genotype, $^{*}P < 0.05$ compared to WT at same stage. *B* and *C*, vasoconstriction in response to 15 mM (*B*) or 50 mM KCl (*C*) in pressurized UAs isolated from NP, P14 or P18 WT (open columns, $n = 7$–9) and BK$_{Ca}^{-/-}$ mice (filled columns, $n = 7$–13). Columns are mean values ± SEM. $^{\dagger}P < 0.05$ compared to NP of the same genotype. *D* and *E*, constriction induced by 1–100 nM IbTX, measured as percentage of diameter after 15 mM KCl-induced vasoconstriction of pressurized UAs from NP, P14 and P18 WT (*D*, $n = 7$–9) and BK$_{Ca}^{-/-}$ mice (*E*, $n = 6$–12). Symbols are mean ± SEM. $^{\#}P < 0.05$ compared to NP and $^{\dagger}P < 0.05$ compared to P14, at same IbTX concentration.

Table 2. UA vascular parameters in NP, P14 and P18 WT mice

	WT dams		
	NP (12)	P14 (12)	P18 (9)
Wall thickness (μm)	31 ± 2.5	42.4 ± 3.9†	40.6 ± 2.7†
Cross-sectional area (10^3 μm^2)	34.7 ± 4.8	64.8 ± 5.9†	70.5 ± 5.2†
Wall:lumen ratio	11.3 ± 1.6	10.2 ± 1.4	7.5 ± 0.5†

Data are means ± SEM and number of vessels are in parentheses. $^{\dagger}P < 0.05$ compared to NP. 2-way ANOVA, Sidak.

channels attenuated the vasoconstriction associated with depolarization of UAs in pregnant mice. We observed no differences between genotypes or pregnancy stages at high depolarization levels obtained at a higher KCl concentration (50 mM, Fig. 3*C*), indicating that the BK$_{Ca}$ effect might be masked at higher KCl concentrations.

We next treated isolated UAs with 15 mM KCl, causing 20–40% constriction and ensuring activation of BK$_{Ca}$ channels, and then treated them with the BK$_{Ca}$ inhibitor IbTX, which produced a ∼15% reduction in diameter of pre-constricted UAs from NP WT mice (Fig. 3*D*). Increasing concentrations of IbTX induced a progressive decrease in diameter of UAs from P14 mice (19.3 ± 3.7%, 27.9 ± 6.8% and 33.4 ± 8.4%, with 1, 10 and 100 nM IbTX, respectively, Fig. 3*D*). However, in UAs from P18 mice, all IbTX concentrations evoked a similar larger constriction (51.2 ± 11.4%, 51.5 ± 11.3% and 51.3 ± 10.1%, with 1, 10 and 100 nM IbTX, respectively, Fig. 3*D*). These results suggest that UAs from P18 mice have higher IbTX sensitivity than those from NP and P14 mice. As expected, IbTX did not induce significant constrictions of UAs isolated from BK$_{Ca}^{-/-}$ mice, nor did pregnancy change the response (Fig. 3*E*). These results indicate that increased BK$_{Ca}$ channel activity contributes to the maintenance of a larger UA diameter during pregnancy.

BK$_{Ca}$ channel currents in WT UA SMCs

To investigate the mechanism(s) by which BK$_{Ca}$ activity was increased in UAs during pregnancy, we performed patch clamp analysis of single BK$_{Ca}$ channels in UA SMCs isolated from NP, P14 or P18 WT mice (Fig. 4*A*). In NP mice, the BK$_{Ca}$ channel open probability (P_o), in the presence of 10 μM Ca^{2+}, increased with depolarizing voltages. When we fitted the data to the Boltzmann equation, we found a half-maximal activation ($V_{0.5}$) of 4.7 ± 3 mV (Fig. 4*B*). The goodness of fit (R^2) value for the curve fitting was 0.93 and the $V_{0.5}$ values of each patch were tightly clustered (Fig. 4*E*). In contrast, when we performed similar experiments on UA SMCs isolated from P14 and P18 mice, the R^2 values were 0.81 and 0.76, respectively, indicating poor fits, and the

Table 3. UA vascular parameters in NP, P14 and P18 $BK_{Ca}^{-/-}$ and $\gamma1^{-/-}$ mice

	$BK_{Ca}^{-/-}$ dams			$\gamma1^{-/-}$ dams		
	NP (8)	P14 (9)	P18 (13)	NP (4)	P14 (5)	P18 (6)
Wall thickness (μm)	30.8 ± 1.8	38 ± 2.2	38.7 ± 1.9	30 ± 2.6	36.2 ± 1.2	41.5 ± 3.1
Cross-sectional area (10^3 μm^2)	28.8 ± 2.2	62.2 ± 5.2†	57.7 ± 3.9†	28.8 ± 2.7	53.6 ± 2.8	57.6 ± 5.6†
Wall:lumen ratio	11.8 ± 1.1	8.5 ± 0.5	9.2 ± 0.8	11 ± 1.2	8.3 ± 0.2	10.6 ± 1.1

Data are means ± SEM and number of vessels are in parentheses. †$P < 0.05$ compared to NP of same genotype. 2-way ANOVA, Sidak.

$V_{0.5}$ values appeared to be in three clusters (Fig. 4*E*). When we separately analysed the three clusters, which we termed '*low*', '*mid*' and '*high*' voltage sensitivity, the R^2 values increased. Specifically, at P14, 82% of channels were *low* sensitivity (−5.8 ± 3.1 mV, $R^2 = 0.94$), 9% were *mid* sensitivity (−44.7 mV, $R^2 = 0.98$) and 9% were *high* sensitivity (−82.3 mV, $R^2 = 0.95$) (Fig. 4*C* and *E*). At P18, 68% of channels were *low* sensitivity (−6.1 ± 3.9 mV, $R^2 = 0.89$), 28% were *mid* sensitivity (−39.2 ± 2.3 mV, $R^2 = 0.97$) and 4% were *high* sensitivity (−82.3 mV, $R^2 = 0.99$) (Fig. 4*D* and *E*). We conclude that, at late stages of pregnancy, a subset of BK_{Ca} channels in UA SMCs have increased voltage sensitivity.

Role of BK_{Ca} $\gamma1$-subunit in UA vasodilatation during pregnancy

Because the BK_{Ca} $\gamma1$-subunit increases the voltage sensitivity of the BK_{Ca} channel in SMCs from cerebral arteries (Evanson *et al.* 2014), we wondered whether the $\gamma1$-subunit contributed to BK_{Ca} channel activity in UA SMCs during pregnancy. Thus, we analysed mRNA expression of BK_{Ca} α-, $\beta1$- and $\gamma1$-subunits in UAs from NP, P14 and P18 mice. mRNA expression levels of α- and $\beta1$-subunits did not differ in UA SMCs from NP and pregnant animals nor change with advancing gestation (Fig. 5*A* and *B*). However, the mRNA expression levels of the $\gamma1$-subunit in UAs from P14 and P18 mice were 9.6- and 6.8-fold greater, respectively, than in those from NP mice (Fig. 5*C*).

To determine the contribution of the $\gamma1$-subunit to UA diameter during pregnancy, we used four approaches. First, we delivered control scrambled (Scr) shRNA or $\gamma1$ shRNA into UAs from P14 and P18 WT mice to determine whether disruption of the $\gamma1$-subunit decreased basal UA diameter. The $\gamma1$ shRNA lowered transcript levels of $\gamma1$ (46 ± 13% of Scr shRNA levels, $P < 0.05$) but had no effect on α- or $\beta1$-subunit transcript levels (78 ± 15% and 97 ± 22%, respectively, of Scr shRNA levels). We found that basal UA diameter was smaller in the P14 and P18 UAs treated with either Scr or $\gamma1$ shRNAs than in non-permeabilized UAs (compare Fig. 6*A*–*C* to Fig. 3*A*), indicating that shRNA delivery affected basal UA diameter non-specifically. However, the basal diameters of UAs treated with $\gamma1$ or Scr shRNAs were equivalent (Fig. 6*A* and *C*), indicating that $\gamma1$ did not contribute to basal diameter.

As a second approach to assess $\gamma1$ function, we knocked down $\gamma1$-subunit expression and examined the effect of the BK_{Ca} inhibitor IbTX on UA diameter. If the $\gamma1$-subunit was required for BK_{Ca} function, then, as we saw with UAs from $BK_{Ca}^{-/-}$ mice (Fig. 3*E*), UAs should be less sensitive to IbTX and show a smaller decrease in diameter. Consistent with this, we found that both P14 and P18 UAs transfected with Scr shRNA constricted in response to IbTX, but those transfected with $\gamma1$ shRNA had an attenuated response to IbTX at P14 and P18 (Fig. 6*B* and *D*). As expected, transfection of P18 UAs with BK_{Ca} shRNAs had no effect on basal diameter, but reduced the constriction in response to IbTX (Fig. 6*E* and *F*).

As a third approach to assess $\gamma1$ function, we overexpressed the $\gamma1$-subunit in NP UAs, reasoning that it should increase sensitivity to BK_{Ca} channel inhibition with IbTX. NP UAs in which the $\gamma1$-subunit was overexpressed had equivalent basal diameter to those transfected with an empty vector (Fig. 6*G*). However, NP UAs in which the $\gamma1$-subunit was overexpressed had significantly larger IbTX-induced contractions than those transfected with the empty vector (Fig. 6*H*). In comparing Fig. 6*H* to Fig. 3*D*, we conclude that overexpression of the $\gamma1$-subunit in NP UAs activated BK_{Ca} to a level similar to that measured in P14 UAs.

As a final approach to assess $\gamma1$ function, we examined UA function during pregnancy in $\gamma1$-subunit knockout ($\gamma1^{-/-}$) mice. UA basal diameter was similar between NP $\gamma1^{-/-}$ mice and WT mice (275 ± 16.8 μm and 281 ± 19.2 μm, Fig. 7*A*). UA diameters increased during pregnancy and were similar between $\gamma1^{-/-}$ and WT mice at P14 (435.2 ± 9.1 μm and 448.3 ± 24.8 μm, Fig. 7*A*). However, at P18, UA basal diameters were significantly smaller in $\gamma1^{-/-}$ mice than in WT mice (400.5 ± 24.9 μm *vs.* 584.1 ± 18.1 μm, $P < 0.05$, Fig. 7*A*). Moreover, IbTX did not induce significant constrictions of UAs isolated from $\gamma1^{-/-}$ mice, nor did pregnancy change the response (Fig. 7*B*). UA structural measurements, such as wall thickness, cross-sectional area and wall:lumen ratio were similar between WT and $\gamma1^{-/-}$ mice (Tables 2 and 3). Finally, $\gamma1^{-/-}$ mice had significantly fewer pups per litter

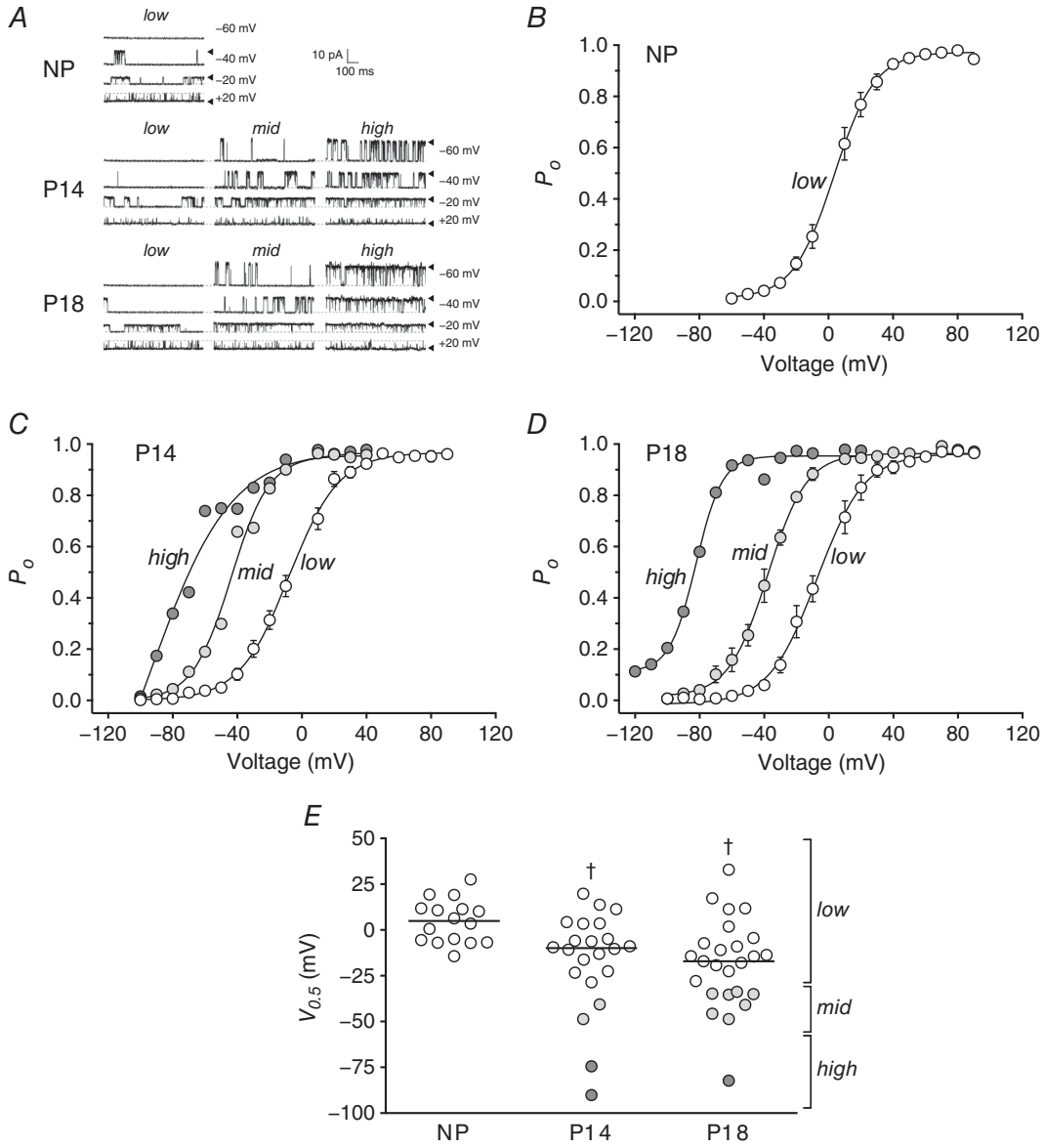

Figure 4. BK_{Ca} single-channel voltage activation in UA SMCs from WT mice
A, representative inside-out patch-clamp recordings from UA SMCs isolated from NP, P14 and P18 WT mice in the presence of 10 μM Ca^{2+} in the bath; membrane potential was held as indicated. Arrowheads and dashed lines indicate open and closed states of the channels, respectively. Single-channel currents from NP, P14 and P18 showed different activation patterns (*low*, *mid* and *high*). *B–D*, voltage dependence of BK_{Ca} channel activation in UA SMCs isolated from NP (*B*), P14 (*C*) and P18 mice (*D*), expressed as open probability of the channel (P_o), in the presence of 10 μM Ca^{2+}. Single-channel currents from NP, P14 and P18 showed different activation voltages, shown as different curves (*low*, *mid* and *high*; open, light grey and dark grey circles, respectively). Symbols are mean values ± SEM, except where $n = 1$ or 2. *E*, voltage of half-maximal activation ($V_{0.5}$) obtained from voltage-activation curves from NP (circles, $N = 4$ mice), P14 (squares, $N = 9$ mice) and P18 mice (triangles, $N = 11$ mice). Three sensitivities to voltage (*low*, *mid* and *high*) are depicted by open, light grey and dark grey circles, respectively. In P14, *low* sensitivity values were measured in 18 patches from 8 mice (mice 1, 2, 4, 5, 6, 7, 8, 9), *mid* sensitivity values were observed in 2 patches from 2 mice (mice 1 and 8) and *high* sensitivity values were measured in 2 patches from 2 mice (mice 1 and 3). In P18, *low* sensitivities were observed in 16 patches from 10 mice (mice 10, 11, 12, 13, 15, 16, 17, 18, 19, 20), *mid* sensitivity values were found in 7 patches from 6 mice (mice 14, 15, 16, 17, 18, 19) and *high* sensitivity was observed in 1 patch from 1 mouse (mouse 20). Symbols are individual patches; lines are median values. $^{\dagger}P < 0.05$ compared to NP.

than WT mice (6.4 ± 0.8 *vs.* 8.4 ± 0.3, $P < 0.05$). In all of these assays, the effects of loss of γ1 were similar to the effects of loss of BK_{Ca} (compare to Fig. 3*A* and *E* and $BK_{Ca}^{-/-}$ data in Tables 1 and 3). Together, these results suggest that the enhanced BK_{Ca} activity observed in UAs from pregnant mice was, in part, due to modulation by the γ1-subunit.

Discussion

The UA undergoes significant vasodilatation and remodelling during gestation, resulting in increased blood flow and supply of nutrients and oxygen to the developing fetus (Osol & Cipolla, 1993; Osol & Moore, 2014). Here, we present several lines of evidence that the BK_{Ca} channel and its auxiliary γ1-subunit contribute to pregnancy-dependent increases in UA diameter and blood flow in mice. First, *in vitro* analysis revealed that UA diameter steadily increased during pregnancy in WT mice. Second, both myography and electrophysiological analyses showed that BK_{Ca} channel activity increased in the UA during pregnancy. Finally, mice lacking either the BK_{Ca} channel α-subunit or γ1-subunit had reduced UA diameters at late pregnancy (P18).

Our results are consistent with the proposal that the BK_{Ca} channel attenuates vascular SMC contractions. In vascular SMCs, BK_{Ca} channel activity repolarizes the membrane potential after Ca^{2+}-mediated depolarization, inactivating voltage-dependent Ca^{2+} channels and causing blood vessels to dilate (Brayden & Nelson, 1992; Nelson *et al.* 1995). Thus, the increased BK_{Ca} channel activity we observed in UAs from pregnant mice likely induces hyperpolarization of the SMC membrane, leading to UA vasodilatation. Future studies using sharp electrode recordings in intact UAs, or current-clamp recordings or membrane potential-sensitive dyes in isolated SMCs might elucidate the effect of pregnancy on the UA SMC membrane potential and the role of the BK_{Ca} channel in this regulation. Moreover, studies exploring Ca^{2+} dynamics in isolated UAs or individual SMCs at different stages of pregnancy could elucidate whether changes in Ca^{2+} sparks coupled to BK_{Ca}-dependent spontaneous transient outward currents, as shown in other vascular beds (Jaggar *et al.* 2000), contribute to pregnancy-dependent vasodilatation of UAs.

In SMCs, as in other cell types, BK_{Ca} channel voltage and Ca^{2+} sensitivity are modulated by the auxiliary β-subunit. The β1-subunit helps regulate vascular tone (Brenner *et al.* 2000; Leo *et al.* 2014), as evidenced by the fact that β1 knockout mice have altered myogenic tone and high blood pressure (Brenner *et al.* 2000; Pluger *et al.* 2000). In the UA, β1-subunit protein expression is higher in pregnant sheep than in non-pregnant animals (Rosenfeld *et al.* 2009; Hu *et al.* 2011) as a result of 17β-oestradiol (Nagar *et al.* 2005; Hu *et al.* 2011) and epigenetic regulation of the β1-subunit gene promoter (Chen *et al.* 2014), suggesting one mechanism to enhance activity of the BK_{Ca} channel.

BK_{Ca} is also regulated by the γ1-subunit in other cell types. For example, in prostate cancer cells, the γ1-subunit increases the voltage sensitivity of BK_{Ca} and allows its activation at resting membrane potential and low intracellular Ca^{2+} concentrations (Yan & Aldrich, 2010). Recently, Evanson *et al.* (2014) showed that the γ1-subunit can increase both BK_{Ca} channel activity in vascular SMCs and BK_{Ca}-induced vasodilatation of cerebral arteries (Evanson *et al.* 2014). Here, we found that knockdown of the γ1-subunit partially reduced BK_{Ca} channel activity in UAs from P14 and P18 mice. Conversely, overexpression of the γ1-subunit increased activity of the channel in UAs from NP mice. Confirming these findings, we found that UAs from $\gamma 1^{-/-}$ P18 mice had smaller diameters and lower BK_{Ca} activity, measured as response to IbTX, than those from WT P18 mice. These observations suggest that the γ1-subunit is, in part, responsible for the enhanced activation of BK_{Ca} channels and likely contributes to

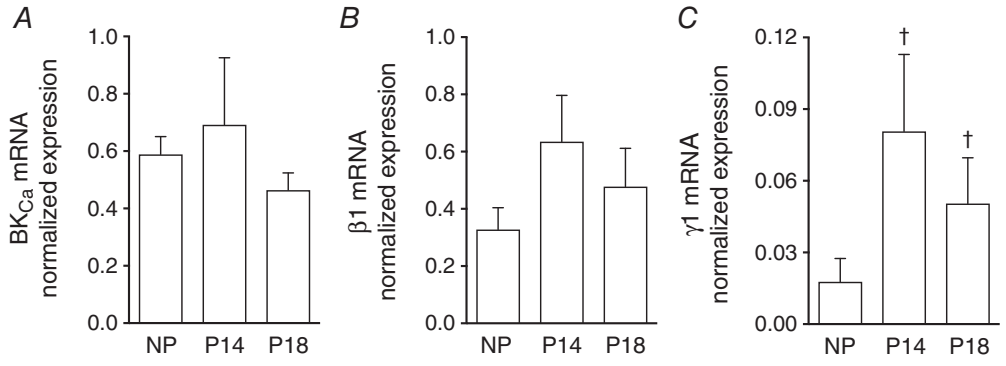

Figure 5. mRNA expression of BK_{Ca} and its auxiliary β1- and γ1-subunits in UA during pregnancy
qPCR analysis of mRNA levels from BK_{Ca} α- (*A*, n = 6–10), β1- (*B*, n = 5–7) and γ1-subunits (*C*, n = 6–8) in UAs isolated from NP, P14 and P18 WT mice. mRNA expression was normalized to expression of succinate dehydrogenase complex flavoprotein subunit A. Columns are mean values ± SEM. $^{\dagger}P < 0.05$ compared to NP.

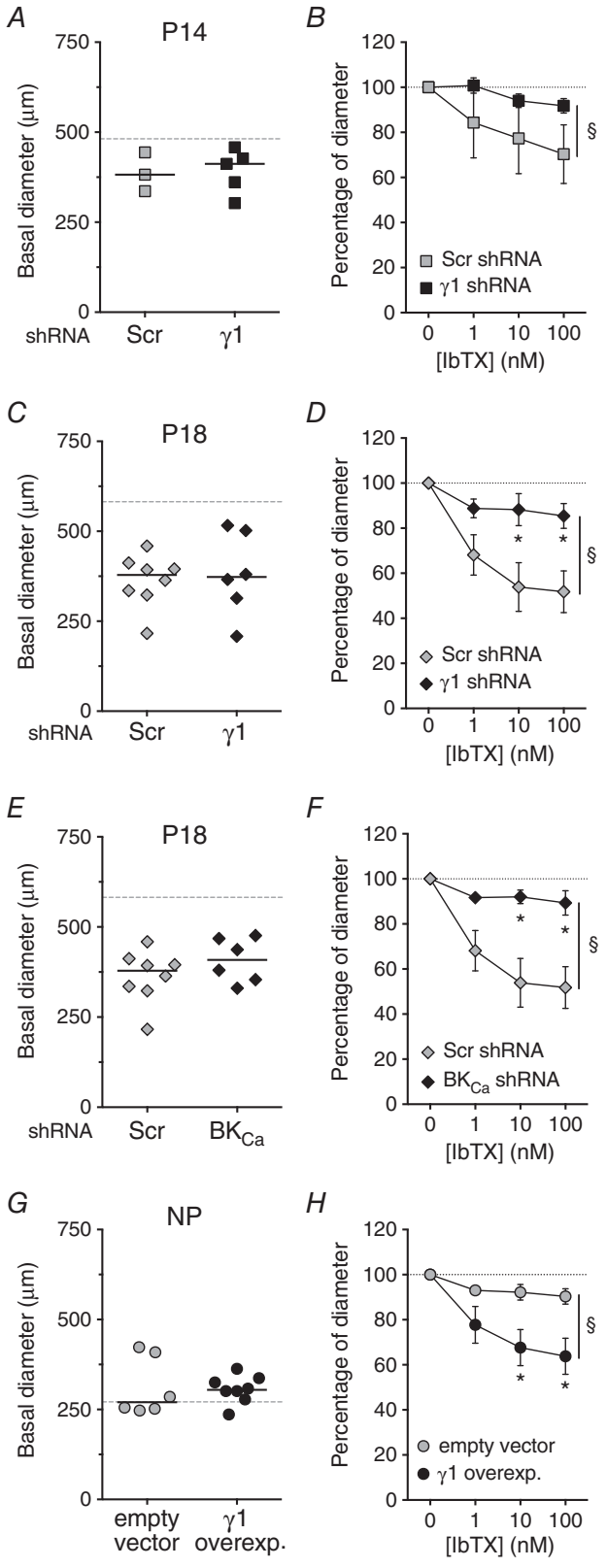

Figure 6. Functional knockdown or overexpression of BK_{Ca} channel γ1-subunits in UAs isolated from pregnant or non-pregnant mice

Basal lumen diameters and 1–100 nM IbTX responses of pressurized UAs from P14 (*A* and *B*), P18 (*C–F*) and NP (*G* and *H*) mice transfected with either Scr (grey symbols, *A–F*), empty vector (grey symbols, *G* and *H*), γ1-subunit-targeted shRNA (filled symbols, *A–D*), BK_{Ca}-targeted shRNA (filled symbols, *E* and *F*) or γ1-subunit overexpression construct (filled symbols, *G* and *H*). Grey dashed lines represent median diameter values of non-permeabilized UAs, as shown in Fig. 3*A*. Symbols in *A*, *C*, *E* and *G* are individual values, bars are median values. Symbols in *B*, *D*, *F* and *H* are mean ± SEM. $^{*}P < 0.05$ compared to Scr shRNA or empty vector at same IbTX concentration, $^{§}P < 0.05$ between curves. P14 (*B*, $n = 3$–5), P18 (*D* and *F*, $n = 6$–8) and NP (*H*, $n = 8$).

the resulting vasodilatation of the UA during pregnancy. Consistent with this idea, we found that the level of γ1 mRNA was higher in UAs from P14 and P18 mice than in those from NP mice. Unfortunately, we were unable to measure the level of γ1-subunit protein or its association with BK_{Ca} during pregnancy because we lacked a sufficiently sensitive antibody. Future immunoblot and protein–protein interaction studies might reveal whether γ1-subunit interaction with BK_{Ca} channel increases in UAs during pregnancy. Both oestrogen and progesterone increase the expression of the β1-subunit in UAs (Nagar *et al.* 2005; Hu *et al.* 2011); thus, γ1 expression might also be hormonally regulated in UAs during pregnancy.

We speculate that the *mid* and *high* voltage sensitivities we observed in UA SMCs at P14 and P18 were due to the association of BK_{Ca} with the β1- and γ1-subunits, respectively. The *mid* voltage sensitive channels were activated with a $V_{0.5}$ around −40 mV, which is comparable to that found in plasma membrane patches containing BK_{Ca} α- and β1-subunits (Lippiat *et al.* 2003; Liu *et al.* 2014; Lorca *et al.* 2014). Although β1-subunit mRNA levels in UAs did not significantly differ between NP, P14 and P18 mice, β1-subunit protein levels may differ. For instance, the β1 protein level increases in UAs from pregnant sheep without significant change in mRNA level (Rosenfeld *et al.* 2009). The *high* voltage sensitive channels were activated with a $V_{0.5}$ around −80 mV, similar to that observed in the presence of the γ1-subunit in other cell types (Yan & Aldrich, 2010, 2012). However, we note that the difference in γ1-subunit mRNA level between UAs from pregnant and non-pregnant mice is much bigger than the difference in numbers of *low*, *mid* and *high* voltage sensitivity channels. This may be because we extracted mRNA from whole UAs pooled from several mice but performed patch clamp on only a few cells within each UA.

Another limitation of our study is the apparent discrepancy between our *in vivo* and *in vitro* data. Given our finding that *in vivo* UA resistance was similar between $BK_{Ca}^{-/-}$ and WT mice at P18, we expected to find that *in vitro* UA diameters would be similar. Instead, UA diameter was smaller in $BK_{Ca}^{-/-}$ than in WT mice at P18. This difference could be due to the influence of the

endothelium, which influences adaptation of the UA to pregnancy (Bird *et al.* 2000). The endothelium produces relaxing factors such as prostaglandins, nitric oxide and endothelial-derived hyperpolarizing factor, all of which modulate BK_{Ca} channels in vascular SMCs (Tanaka *et al.* 2004). Thus, we specifically removed the endothelium for our *in vitro* studies to assess effects of BK_{Ca} on the smooth muscle layer. The fact that UA resistance did not increase as UA diameter decreased in $BK_{Ca}^{-/-}$ mice could indicate structural changes in arterioles, spiral arteries or placental vasculature, which could be assessed by microcomputed tomography. In this context, in mice, placentas become progressively thicker from P10.5 to around P14, then thickness remains constant until term (Mu *et al.* 2008). Our ultrasound studies confirmed that placental thickness in WT mice did not differ between P14 and P18. However, placentas in P18 $BK_{Ca}^{-/-}$ dams were thicker than those in P14 dams, suggesting differential placental growth. Given that performing Doppler imaging of UAs in NP mice is technically demanding, we were unable to measure UA vascular resistance in NP animals. Thus, we could not determine whether the lower UA resistance observed in $BK_{Ca}^{-/-}$ mice than in WT mice at P14 was specific to pregnancy or reflected an overall lower UA resistance in $BK_{Ca}^{-/-}$ mice. Another possibility is that compensation by other ion channels maintains a low UA resistance during pregnancy. Supporting this idea, a reduction in L-type Ca^{2+} currents and increase in protein kinase A expression have been described in urinary bladder SMCs from global $BK_{Ca}^{-/-}$ mice, but not in mice with inducible SMC-specific deletion of BK_{Ca} channels (Sprossmann *et al.* 2009). Thus, it is possible that compensatory mechanisms are also present in vascular SMCs in $BK_{Ca}^{-/-}$ mice.

Throughout pregnancy, both functional vasodilatation and structural remodelling result in changes in UA blood flow. Structural remodelling involves an increase in UA diameter (Cipolla & Osol, 1994; Hilgers *et al.* 2003; Mu & Adamson, 2006). In mice, the increase in UA diameter during pregnancy is accompanied by an increase in wall thickness and SMC hyperplasia (van der Heijden *et al.* 2005), and BK_{Ca} channels have been proposed to regulate cell proliferation (Bloch *et al.* 2007; Coiret *et al.* 2007). We observed a pregnancy-dependent increase in the UA wall thickness in WT mice, but we did not find differences in wall thickness between NP and any pregnant stage in $BK_{Ca}^{-/-}$ mice, suggesting that this channel could play a role in the pregnancy-induced hyperplasia of the UA SMCs and the resulting structural remodelling of these vessels.

Previous studies have shown that abnormal utero-placental perfusion, due to reduced adaptation and/or dysfunction of the UA, contributes to the development of IUGR in humans (Konje *et al.* 2003) and rodents (Cotechini *et al.* 2014; Janot *et al.* 2014). In mice, bilateral ligation of the UA is a proposed model of IUGR (Janot *et al.* 2014), whereas in humans, women with lower uterine artery blood flow are at increased risk of developing IUGR and adverse pregnancy outcomes (Konje *et al.* 2003; Shwarzman *et al.* 2013). Here, we found that loss of BK_{Ca} did not affect pup size, measured as crown–rump length by ultrasound, a good predictor of fetal body weight and gestational age in mice (Mu *et al.* 2008). This is in contrast to an earlier report that $BK_{Ca}^{-/-}$ pups were smaller than their WT littermates (Meredith *et al.* 2004). However, in our study, all pups from WT or $BK_{Ca}^{-/-}$ dams were WT or $BK_{Ca}^{+/-}$, respectively, indicating that loss of one copy of BK_{Ca} is insufficient to reduce pup size. Although fetal sizes were similar between the genotypes, the $BK_{Ca}^{-/-}$ dams had fewer pups than WT dams. A reduced number of pups, and hence lower UA resistance, could overcome the altered utero-placental perfusion due to dysfunction in UA vasodilatation. Further studies might elucidate whether the decreased pup number reflects a defect in implantation or increased resorption in response to abnormal UA flow.

In this study, we described a key role of the BK_{Ca} channel in modulating UA diameter changes at late pregnancy in mice. We proposed that the γ1-subunit participates in this process by increasing the activation of BK_{Ca} channels during pregnancy. Understanding the mechanisms underlying the functional and structural remodelling of the UA during pregnancy might contribute to the development of strategies to prevent dysfunctions of UA remodelling, which is essential for proper fetal development and maternal health.

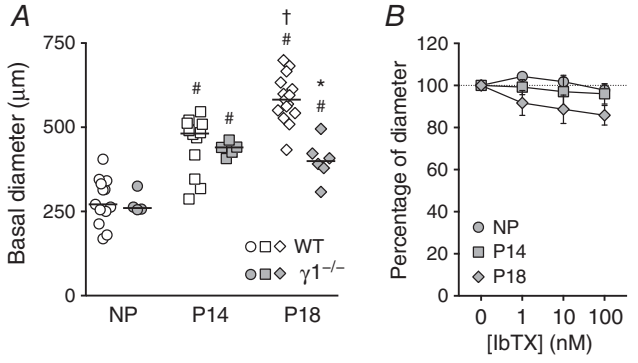

Figure 7. UA lumen diameter and IbTX responses in UAs from γ1-subunit knockout ($\gamma1^{-/-}$) pregnant mice
A, basal lumen diameter of pressurized UAs (60 mmHg) from NP, P14 and P18 WT (open symbols, same data as shown in Fig. 3*A*) or $\gamma1^{-/-}$ mice (grey symbols). Symbols are individual values; bars are median values. $^{\dagger}P < 0.05$ compared to NP of same genotype, $^{\#}P < 0.05$ compared to P14 of same genotype, $^{*}P < 0.05$ compared to WT at same stage. *B*, 1–100 nM IbTX-induced constriction, measured as percentage of diameter after 15 mM KCl-induced vasoconstriction of pressurized UAs from NP, P14 and P18 $\gamma1^{-/-}$ mice (grey symbols, $n = 4$–6). Symbols are mean ± SEM.

References

Alioua A, Lu R, Kumar Y, Eghbali M, Kundu P, Toro L & Stefani E (2008). Slo1 caveolin-binding motif, a mechanism of caveolin-1-Slo1 interaction regulating Slo1 surface expression. *J Biol Chem* **283**, 4808–4817.

Bird IM, Sullivan JA, Di T, Cale JM, Zhang L, Zheng J & Magness RR (2000). Pregnancy-dependent changes in cell signaling underlie changes in differential control of vasodilator production in uterine artery endothelial cells. *Endocrinology* **141**, 1107–1117.

Bloch M, Ousingsawat J, Simon R, Schraml P, Gasser TC, Mihatsch MJ, Kunzelmann K & Bubendorf L (2007). KCNMA1 gene amplification promotes tumor cell proliferation in human prostate cancer. *Oncogene* **26**, 2525–2534.

Brainard AM, Miller AJ, Martens JR & England SK (2005). Maxi-K channels localize to caveolae in human myometrium: a role for an actin-channel-caveolin complex in the regulation of myometrial smooth muscle K^+ current. *Am J Physiol Cell Physiol* **289**, C49–C57.

Brayden JE & Nelson MT (1992). Regulation of arterial tone by activation of calcium-dependent potassium channels. *Science* **256**, 532–535.

Brenner R, Perez GJ, Bonev AD, Eckman DM, Kosek JC, Wiler SW, Patterson AJ, Nelson MT & Aldrich RW (2000). Vasoregulation by the β1 subunit of the calcium-activated potassium channel. *Nature* **407**, 870–876.

Browne VA, Toledo-Jaldin L, Davila RD, Lopez LP, Yamashiro H, Cioffi-Ragan D, Julian CG, Wilson MJ, Bigham AW, Shriver MD, Honigman B, Vargas E, Roach R & Moore LG (2011). High-end arteriolar resistance limits uterine artery blood flow and restricts fetal growth in preeclampsia and gestational hypertension at high altitude. *Am J Physiol Regul Integr Comp Physiol* **300**, R1221–R1229.

Chen M, Dasgupta C, Xiong F & Zhang L (2014). Epigenetic upregulation of large-conductance Ca^{2+}-activated K^+ channel expression in uterine vascular adaptation to pregnancy. *Hypertension* **64**, 610–618.

Cheranov SY & Jaggar JH (2004). Mitochondrial modulation of Ca^{2+} sparks and transient KCa currents in smooth muscle cells of rat cerebral arteries. *J Physiol* **556**, 755–771.

Chiswick ML (1985). Intrauterine growth retardation. *Br Med J (Clin Res Ed)* **291**, 845–848.

Cipolla M & Osol G (1994). Hypertrophic and hyperplastic effects of pregnancy on the rat uterine arterial wall. *Am J Obstet Gynecol* **171**, 805–811.

Coiret G, Borowiec AS, Mariot P, Ouadid-Ahidouch H & Matifat F (2007). The antiestrogen tamoxifen activates BK channels and stimulates proliferation of MCF-7 breast cancer cells. *Mol Pharmacol* **71**, 843–851.

Cotechini T, Komisarenko M, Sperou A, Macdonald-Goodfellow S, Adams MA & Graham CH (2014). Inflammation in rat pregnancy inhibits spiral artery remodeling leading to fetal growth restriction and features of preeclampsia. *J Exp Med* **211**, 165–179.

Curley M, Morrison JJ & Smith TJ (2004). Analysis of Maxi-K alpha subunit splice variants in human myometrium. *Reprod Biol Endocrinol* **2**, 67.

Evanson KW, Bannister JP, Leo MD & Jaggar JH (2014). LRRC26 is a functional BK channel auxiliary gamma subunit in arterial smooth muscle cells. *Circ Res* **115**, 423–431.

Ford SP (1982). Control of uterine and ovarian blood flow throughout the estrous cycle and pregnancy of ewes, sows and cows. *J Anim Sci* **55**, Suppl. 2, 32–42.

Gutkowska J, Jankowski M, Lambert C, Mukaddam-Daher S, Zingg HH & McCann SM (1997). Oxytocin releases atrial natriuretic peptide by combining with oxytocin receptors in the heart. *Proc Natl Acad Sci USA* **94**, 11704–11709.

Hilgers RH, Bergaya S, Schiffers PM, Meneton P, Boulanger CM, Henrion D, Levy BI & De Mey JG (2003). Uterine artery structural and functional changes during pregnancy in tissue kallikrein-deficient mice. *Arterioscler Thromb Vasc Biol* **23**, 1826–1832.

Hu XQ, Xiao D, Zhu R, Huang X, Yang S, Wilson S & Zhang L (2011). Pregnancy upregulates large-conductance Ca^{2+}-activated K^+ channel activity and attenuates myogenic tone in uterine arteries. *Hypertension* **58**, 1132–1139.

Jackson WF, Huebner JM & Rusch NJ (1997). Enzymatic isolation and characterization of single vascular smooth muscle cells from cremasteric arterioles. *Microcirculation* **4**, 35–50.

Jaggar JH, Porter VA, Lederer WJ & Nelson MT (2000). Calcium sparks in smooth muscle. *Am J Physiol Cell Physiol* **278**, C235–C256.

Janot M, Cortes-Dubly ML, Rodriguez S & Huynh-Do U (2014). Bilateral uterine vessel ligation as a model of intrauterine growth restriction in mice. *Reprod Biol Endocrinol* **12**, 62.

Ketsawatsomkron P, Lorca RA, Keen HL, Weatherford ET, Liu X, Pelham CJ, Grobe JL, Faraci FM, England SK & Sigmund CD (2012). PPARγ regulates resistance vessel tone through a mechanism involving RGS5-mediated control of protein kinase C and BKCa channel activity. *Circ Res* **111**, 1446–1458.

Knaus HG, Folander K, Garcia-Calvo M, Garcia ML, Kaczorowski GJ, Smith M & Swanson R (1994). Primary sequence and immunological characterization of β-subunit of high conductance Ca^{2+}-activated K^+ channel from smooth muscle. *J Biol Chem* **269**, 17274–17278.

Knot HJ & Nelson MT (1998). Regulation of arterial diameter and wall $[Ca^{2+}]$ in cerebral arteries of rat by membrane potential and intravascular pressure. *J Physiol* **508**, 199–209.

Konje JC, Howarth ES, Kaufmann P & Taylor DJ (2003). Longitudinal quantification of uterine artery blood volume flow changes during gestation in pregnancies complicated by intrauterine growth restriction. *BJOG* **110**, 301–305.

Korovkina VP, Fergus DJ, Holdiman AJ & England SK (2001). Characterization of a novel 132-bp exon of the human maxi-K channel. *Am J Physiol Cell Physiol* **281**, C361–C367.

Leo MD, Bannister JP, Narayanan D, Nair A, Grubbs JE, Gabrick KS, Boop FA & Jaggar JH (2014). Dynamic regulation of β1 subunit trafficking controls vascular contractility. *Proc Natl Acad Sci USA* **111**, 2361–2366.

Lesh RE, Somlyo AP, Owens GK & Somlyo AV (1995). Reversible permeabilization. A novel technique for the intracellular introduction of antisense oligodeoxynucleotides into intact smooth muscle. *Circ Res* **77**, 220–230.

Lippiat JD, Standen NB, Harrow ID, Phillips SC & Davies NW (2003). Properties of BK_{Ca} channels formed by bicistronic expression of hSloα and β1–4 subunits in HEK293 cells. *J Membr Biol* **192**, 141–148.

Liu HW, Hou PP, Guo XY, Zhao ZW, Hu B, Li X, Wang LY, Ding JP & Wang S (2014). Structural basis for calcium and magnesium regulation of a large conductance calcium-activated potassium channel with β1 subunits. *J Biol Chem* **289**, 16914–16923.

Lorca RA, Stamnes SJ, Pillai MK, Hsiao JJ, Wright ME & England SK (2014). N-terminal isoforms of the large-conductance Ca^{2+}-activated K^+ channel are differentially modulated by the auxiliary β1-subunit. *J Biol Chem* **289**, 10095–10103.

Lu T, Zhang DM, Wang XL, He T, Wang RX, Chai Q, Katusic ZS & Lee HC (2010). Regulation of coronary arterial BK channels by caveolae-mediated angiotensin II signaling in diabetes mellitus. *Circ Res* **106**, 1164–1173.

McManus OB, Helms LM, Pallanck L, Ganetzky B, Swanson R & Leonard RJ (1995). Functional role of the beta subunit of high conductance calcium-activated potassium channels. *Neuron* **14**, 645–650.

Meredith AL, Thorneloe KS, Werner ME, Nelson MT & Aldrich RW (2004). Overactive bladder and incontinence in the absence of the BK large conductance Ca^{2+}-activated K^+ channel. *J Biol Chem* **279**, 36746–36752.

Mu J & Adamson SL (2006). Developmental changes in hemodynamics of uterine artery, utero- and umbilicoplacental, and vitelline circulations in mouse throughout gestation. *Am J Physiol Heart Circ Physiol* **291**, H1421–H1428.

Mu J, Slevin JC, Qu D, McCormick S & Adamson SL (2008). In vivo quantification of embryonic and placental growth during gestation in mice using micro-ultrasound. *Reprod Biol Endocrinol* **6**, 34.

Nagar D, Liu XT & Rosenfeld CR (2005). Estrogen regulates β_1-subunit expression in Ca^{2+}-activated K^+ channels in arteries from reproductive tissues. *Am J Physiol Heart Circ Physiol* **289**, H1417–H1427.

Nelson MT, Cheng H, Rubart M, Santana LF, Bonev AD, Knot HJ & Lederer WJ (1995). Relaxation of arterial smooth muscle by calcium sparks. *Science* **270**, 633–637.

Osol G & Cipolla M (1993). Pregnancy-induced changes in the three-dimensional mechanical properties of pressurized rat uteroplacental (radial) arteries. *Am J Obstet Gynecol* **168**, 268–274.

Osol G & Moore LG (2014). Maternal uterine vascular remodeling during pregnancy. *Microcirculation* **21**, 38–47.

Palmer SK, Zamudio S, Coffin C, Parker S, Stamm E & Moore LG (1992). Quantitative estimation of human uterine artery blood flow and pelvic blood flow redistribution in pregnancy. *Obstet Gynecol* **80**, 1000–1006.

Pluger S, Faulhaber J, Furstenau M, Lohn M, Waldschutz R, Gollasch M, Haller H, Luft FC, Ehmke H & Pongs O (2000). Mice with disrupted BK channel beta1 subunit gene feature abnormal Ca^{2+} spark/STOC coupling and elevated blood pressure. *Circ Res* **87**, E53–60.

Rada CC, Pierce SL, Nuno DW, Zimmerman K, Lamping KG, Bowdler NC, Weiss RM & England SK (2012). Overexpression of the SK3 channel alters vascular remodeling during pregnancy, leading to fetal demise. *Am J Physiol Endocrinol Metab* **303**, E825–E831.

Rosenfeld CR, Cornfield DN & Roy T (2001). Ca^{2+}-activated K^+ channels modulate basal and $E_2\beta$-induced rises in uterine blood flow in ovine pregnancy. *Am J Physiol Heart Circ Physiol* **281**, H422–H431.

Rosenfeld CR, Liu XT & DeSpain K (2009). Pregnancy modifies the large conductance Ca^{2+}-activated K^+ channel and cGMP-dependent signaling pathway in uterine vascular smooth muscle. *Am J Physiol Heart Circ Physiol* **296**, H1878–H1887.

Rosenfeld CR, Word RA, DeSpain K & Liu XT (2008). Large conductance Ca^{2+}-activated K^+ channels contribute to vascular function in nonpregnant human uterine arteries. *Reprod Sci* **15**, 651–660.

Shwarzman P, Waintraub AY, Frieger M, Bashiri A, Mazor M & Hershkovitz R (2013). Third-trimester abnormal uterine artery Doppler findings are associated with adverse pregnancy outcomes. *J Ultrasound Med* **32**, 2107–2113.

Sprossmann F, Pankert P, Sausbier U, Wirth A, Zhou XB, Madlung J, Zhao H, Bucurenciu I, Jakob A, Lamkemeyer T, Neuhuber W, Offermanns S, Shipston MJ, Korth M, Nordheim A, Ruth P & Sausbier M (2009). Inducible knockout mutagenesis reveals compensatory mechanisms elicited by constitutive BK channel deficiency in overactive murine bladder. *FEBS J* **276**, 1680–1697.

Tanaka Y, Koike K & Toro L (2004). MaxiK channel roles in blood vessel relaxations induced by endothelium-derived relaxing factors and their molecular mechanisms. *J Smooth Muscle Res* **40**, 125–153.

Tanaka Y, Meera P, Song M, Knaus HG & Toro L (1997). Molecular constituents of maxi K_{Ca} channels in human coronary smooth muscle: predominant $\alpha + \beta$ subunit complexes. *J Physiol* **502**, 545–557.

van der Heijden OW, Essers YP, Spaanderman ME, De Mey JG, van Eys GJ & Peeters LL (2005). Uterine artery remodeling in pseudopregnancy is comparable to that in early pregnancy. *Biol Reprod* **73**, 1289–1293.

Yan J & Aldrich RW (2010). LRRC26 auxiliary protein allows BK channel activation at resting voltage without calcium. *Nature* **466**, 513–516.

Yan J & Aldrich RW (2012). BK potassium channel modulation by leucine-rich repeat-containing proteins. *Proc Natl Acad Sci USA* **109**, 7917–7922.

Yang C, Gonzalez-Perez V, Mukaibo T, Melvin JE, Xia XM & Lingle CJ (2017). Knockout of the LRRC26 subunit reveals a primary role of LRRC26-containing BK channels in secretory epithelial cells. *Proc Natl Acad Sci USA* **114**, E3739–E3747.

Zhu N, Eghbali M, Helguera G, Song M, Stefani E & Toro L (2005). Alternative splicing of Slo channel gene programmed by estrogen, progesterone and pregnancy. *FEBS Lett* **579**, 4856–4860.

Additional information

Competing interests

None declared.

Author contributions

R.A.L. and S.K.E. designed the study; R.A.L., M.W.-P., W.E.F. and M.K.P. acquired and analysed the data; R.A.L., M.W.-P. and S.K.E. interpreted the results and wrote the manuscript. All authors have approved the final version of the manuscript and agree to be accountable for all aspects of the work. All persons designated as authors qualify for authorship, and all those who qualify for authorship are listed.

Funding

This work was supported by National Institutes of Health grant 5R01HD037831 and March of Dimes grant FY15-147 to S.K.E., and American Heart Association Postdoctoral fellowship AHA/12POST10660000 to R.A.L.

Acknowledgements

We thank Dr Deborah J. Frank, Dr Kathryn G. Lamping and Dr Lorna G. Moore for critical reading and editing of the manuscript, Dr Molly J. Stout for scientific discussion, Dr Andrea L. Meredith for providing the $BK_{Ca}^{-/-}$ mice, Dr Christopher J. Lingle for providing the $\gamma 1^{-/-}$ mice, Mrs Elise S. Bales for technical assistance with immunohistochemistry studies, the Cardiovascular Mouse Phenotyping Core at Washington University in St Louis for Doppler imaging assistance, and The Genome Institute at Washington University in St Louis for shRNA synthesis.